

Sublinear dispersive conductivity in polyetherimides by the electric modulus formalism

M. Mudarra, J. Sellarès, J. C. Cañadas, J. A. Diego

Dept. Física i Enginyeria Nuclear, Universitat Politècnica de Catalunya,
Campus de Terrassa, C. Colom 11, Terrassa E-08222 (Spain)

E-mail: jordi.sellares@upc.es

Abstract. It can be seen by Dynamic Electrical Analysis that the electrical properties of polyetherimide at temperatures above the glass transition are strongly influenced by space charge. We have studied space charge relaxation in two commercial grades of polyetherimide, Ultem 1000 and Ultem 5000, using this technique. The electric modulus formalism has been used to interpret their conductive properties. In both grades of polyetherimide, asymmetric Argand plots are observed, which are related to a sublinear power-law dependency (ω^n with $n < 1$) in the real part of the conductivity. This behaviour is attributed to correlated ion hopping. The imaginary part of the electric modulus exhibits a peak in the low frequency range associated to conduction. Modelling of this peak allows us to obtain the dependence, among other parameters, of the conductivity (σ_0), the fractional exponent (n) and the crossover frequency (ω_p) on the temperature. The α relaxation, that appears at higher frequencies, has also to be modelled since it overlaps the conductivity relaxation. The study of the parameters in terms of the temperature allows us to identify the ones that are thermally activated. The difference between the conductivity relaxation time and the Maxwell relaxation time indicates the presence of deep traps. The coupling model points out that the correlation of the ionic motion diminishes with temperature, probably due to increasing disorder due to thermal agitation.

PACS numbers: 64.70.Pj, 77.22.Gm, 72.20.-i

1. Introduction

Polyetherimide (PEI) is an amorphous thermoplastic resin with a high glass transition temperature that was developed by General Electric. Because of its advantageous mechanical, thermal, and electrical properties, this resin is suitable for industrial applications, such as microwave devices, high performance electrical devices and biomedical applications. For many of these applications it is important to know the relaxational behaviour of the material to foresee its response. Among these relaxations, those related to space charge play an especially important role in the electrical response of the material.

Our study is focused on two commercial grades of PEI Ultem 1000 and Ultem 5000. These resins have similar chemical structure, but Ultem 1000 is meta-linked whereas

Ultem 5000 is para-linked (Fig. 1). Ultem 5000 has enhanced chemical stability versus acids and organic solvents.

Previous studies show that the dielectric strength of Ultem 5000 is higher than in the case of Ultem 1000 over a wide temperature range and the value of this magnitude diminishes with the temperature in both grades [1]. The differences are attributed to the remnant electrical field due to space charge, as charge injection from the electrode is more efficient in the case of Ultem 1000. Krause, Yang and Sessler have observed that in corona charged samples surface charge decays faster in the case of Ultem 5000 and that this grade is more sensitive to the change of the polarity of the applied field [2]. They attribute these differences to a more continuous band structure due to the existence of an ordered morphology on Ultem 5000 films.

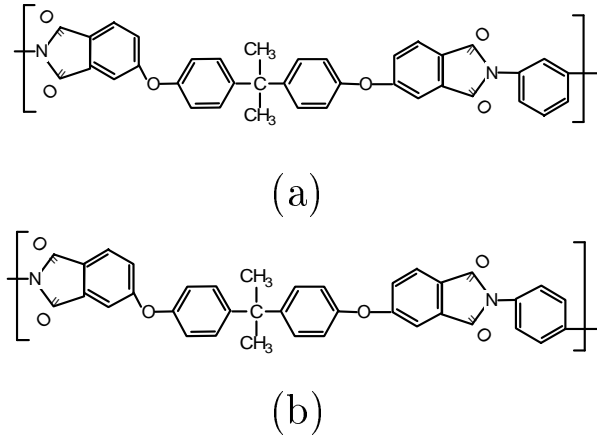


Figure 1. Chemical structures of Ultem 1000 (a) and Ultem 5000 (b)

It is also known that the loss factor of Ultem 1000 increases sharply for temperatures close to the glass transition temperature due to conductive processes [3]. In the case of thermally stimulated depolarization currents (TSDC) measurements, the relaxation of space charge is associated with the ρ relaxation, which appears at temperatures higher than the α relaxation, associated to the glass transition [4]. This peak was studied by means of the general order kinetic model [5, 6, 7, 8], that provides information about the relaxation mechanism for space charge and it was concluded that recombination was the most likely relaxation mechanism and that the depth of the traps is approximately 2.6 eV [4].

In this paper we present a relaxational study of the conductivity of polyetherimide to improve the understanding of the mechanisms related to space charge in this material. The α relaxation has also been studied since both relaxations are so close that they overlap and cannot be studied on their own.

Data will be obtained by means of the dynamic electrical analysis (DEA) technique and interpreted using the electric modulus formalism [9, 10, 11, 12]. The electric modulus

(M^*) can be obtained from the permittivity (ϵ^*) through

$$M^* = (\epsilon^*)^{-1}. \quad (1)$$

The conductivity relaxation appears as a flex in the imaginary part of the permittivity. Instead, in the electric modulus it appears as peak allowing an easier interpretation of the data. The electric modulus formalism has been used to study the conductivity relaxation in polymers [13, 14], glasses [15], crystals [16], ceramics [17] and composites [18, 19], among other materials.

We expect to find a sublinear frequency dispersive AC conductivity as in many other systems [20]. In this case the real part of the conductivity $\sigma'(\omega)$ can be expressed as

$$\sigma'(\omega) = \sigma_0 + A\omega^n \quad (2)$$

where σ_0 is the DC conductivity, A is a temperature dependent parameter and n is a fractional exponent which ranges between 0 and 1 and has been interpreted by means of many body interactions among charge carriers [21].

This behaviour, termed universal dynamic response, has been observed in highly disordered materials like ionically conducting glasses, polymers, amorphous semiconductors and also in doped crystalline solids [15, 16, 19, 22, 23, 24, 25]. Equation 2 can be derived from the universal dielectric response function [26] for the dielectric loss of materials with free hopping carriers.

With regards to the α relaxation, we will consider that the relaxation time follows the Havriliak–Negami equation and has Vogel–Tammann–Fulcher dependence on temperature.

It will be of particular interest to find the dependence of the obtained parameters on the temperature [27]. All in all, the parameters that result from the modelling will allow us to characterize the relaxational behaviour of Ultem 1000 and Ultem 5000 above T_g and to obtain information about the space charge mechanisms in polyetherimide.

2. Experimental

Two grades of PEI, Ultem 1000 and Ultem 5000, were supplied by General Electric. DSC measurements indicate that their glass transition temperatures (T_g) are: $T_g \approx 220$ °C in the case of Ultem 1000 and $T_g \approx 235$ °C for ultem 5000.

Samples of Ultem 1000 and Ultem 5000 were cut from sheets of 125 μm in square portions with a side of 25 mm. The samples were placed between gold plated electrodes with radius 20 mm and measured using a Novocontrol BDS40 dielectric spectrometer with a Novotherm temperature control system.

The real and imaginary parts of the electrical permittivity were measured at several frequencies between 10^{-2} Hz and 10^6 Hz at isothermal steps of 5 °C each at temperatures ranging between 230 °C and 285 °C in the case of Ultem 1000 and between 255 °C and 290 °C in the case of Ultem 5000. These temperature ranges are above the respective

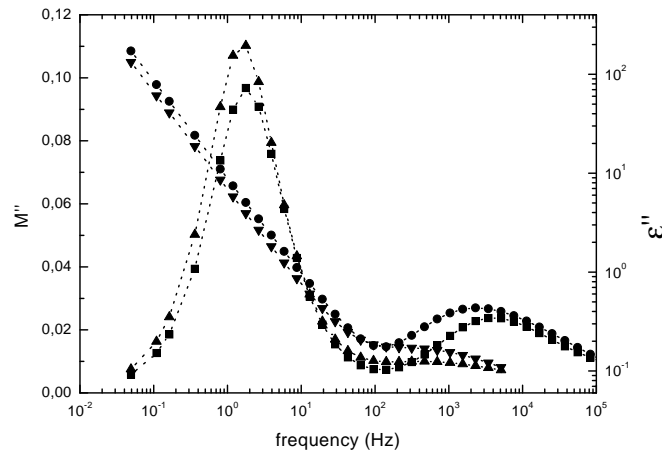


Figure 2. Imaginary part of the electric modulus at $T = 255$ °C of Ultem 1000 (■) and Ultem 5000 (▲). Loss factor of Ultem 1000 (●) and Ultem 5000 (▼) at the same temperature.

glass transition of the PEI grades in order to get a substantial contribution of the conductive processes.

3. Results and discussion

The loss factor (ϵ'') and the imaginary part of the electric modulus (M'') of Ultem 1000 and Ultem 5000 are plotted in figure 2 as a function of the frequency for a temperature $T = 255$ °C, which lies above T_g in both cases. It can be seen that the conductive processes in both materials result in a sharp increase of the loss factor at low frequencies. In the case of the imaginary part of the electric modulus, these effects are evidenced by a peak. This is certainly easier to model [12, 28]. For this reason we have choosed the electric modulus formalism to study the conduction relaxation.

In figure 3 we have plotted the electric modulus in Argand's plane, for temperatures close to the glass transition temperature of Ultem 1000. The corresponding plots of the electric modulus show two arcs, i.e., the conductive processes result in an arc for low frequencies and for higher frequencies we can observe another arc that can be associated with the α relaxation. Depressed arcs are observed in the case of the relaxation associated with conductive processes that can be related to a dispersive regime [29].

In figure 4 we have plotted the peak associated with the conductive process in Ultem 1000 for several temperatures above the glass transition. It can be noted that the peak shifts to higher frequencies with the temperature.

To study the charge transport process at these temperatures we have assumed a sublinear frequency dispersive AC conductivity, as depressed arcs observed in figure 3 for low frequencies can be associated with a dispersive regime. Power-law dependencies of conductivity, as in the case of equation 2, imply a power-law dependence of the form

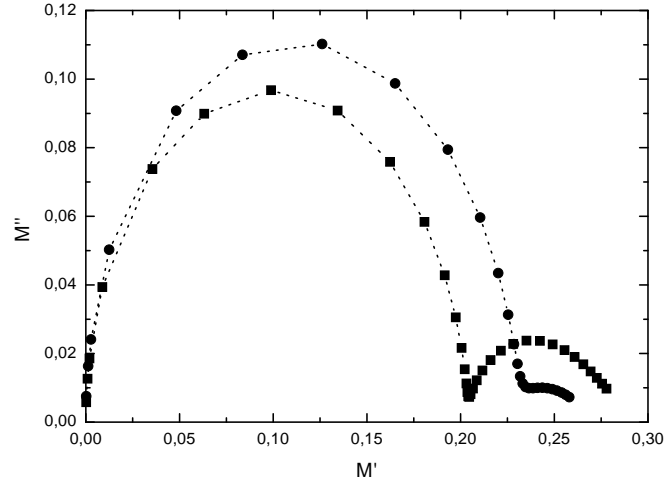


Figure 3. Argand's plot of the electric modulus M^* of Ultem 1000 (■) and Ultem 5000 (●) at $T = 255$ °C. (Frequency of plotted data increases from left to right)

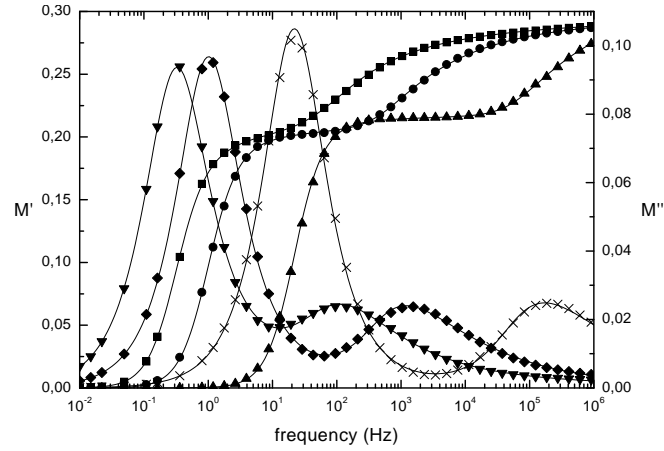


Figure 4. Real and Imaginary parts of the electric modulus of Ultem 1000 versus the frequency for several temperatures. Real part: ■, 240 °C; ●, 250 °C; ▲, 280 °C; Imaginary part: ▼, 240 °C; ◆, 250 °C; ×, 280 °C. The symbols are measured values and the continuous curves are the calculated values using the values of table 1 resulting from the fitting process to equation 9

$(j \omega)^n$ for the complex conductivity[30]. Therefore, this magnitude can be written:

$$\sigma^*(\omega) = \sigma_0 + A(j \omega)^n + j \omega \varepsilon_0 \varepsilon_{\infty C} \quad (3)$$

where $\varepsilon_{\infty C}$ refers to the permittivity at high frequency. A crossover frequency ω_p can be defined as

$$\omega_p^n \equiv \sigma_0 / A \quad (4)$$

so that equation 3 can be rewritten as

$$\sigma^*(\omega) = \sigma_0 + \sigma_0 \left(j \frac{\omega}{\omega_p} \right)^n + j \omega \varepsilon_0 \varepsilon_{\infty C} \quad (5)$$

This frequency ω_p is associated with the crossover from the power-law dependence observed at high frequency to a frequency independent DC regime that occurs at low frequencies. Finally the contribution to the permittivity is

$$\varepsilon_C^* = -\frac{j\sigma^*}{\varepsilon_0\omega} \quad (6)$$

The α relaxation can be modeled by means of Havriliak-Negami equation

$$\varepsilon_{HN}^* = \varepsilon_{\infty HN} + \frac{\Delta\varepsilon}{(1 + (j\omega\tau_{HN})^{\alpha_{HN}})^{\beta_{HN}}} \quad (7)$$

where $\varepsilon_{\infty HN}$ refers to the permittivity at high frequencies and

$$\Delta\varepsilon = \varepsilon_{\infty C} - \varepsilon_{\infty HN} \quad (8)$$

is the relaxation strength. Therefore the electric modulus over the frequency range considered can be expressed as:

$$M^* = (\varepsilon_C^* + \varepsilon_{HN}^*)^{-1} \quad (9)$$

Electric modulus versus frequency data have been fitted to equation 9. The real and imaginary parts of the electric modulus, $M^*(\omega)$, were calculated from the complex permittivity and were fitted to the real and imaginary parts of the electric modulus given by equation 9 simultaneously. Eight independent parameters were used in the fitting process: σ_0 , ω_p , $\varepsilon_{\infty C}$, n , $\varepsilon_{\infty HN}$, τ_{HN} , α_{HN} and β_{HN} .

The study of the two contributions to electric modulus, given by equation 6 and equation 7, indicates that the first contribution (which is characterized by four of the parameters: σ_0 , ω_p , $\varepsilon_{\infty C}$, n) helps to explain appropriately the contribution of conductive processes, whereas that the second contribution (which is characterized by the four remaining parameters, $\varepsilon_{\infty HN}$, τ_{HN} , α_{HN} and β_{HN}) explains main relaxation α . Both contributions are plotted separately in figure 5. It can be noted that each process (and, therefore, each set of four parameters) mainly contributes in a different frequency range, and the whole set of eight parameters is required to explain adequately the experimental response observed over the whole frequency range.

In this work we have used simulated annealing to carry out the fitting process. This method has been successfully used in the analysis of thermally stimulated depolarization currents [31, 32] and dielectric spectroscopy data [33]. The values of the parameters obtained are shown in tables 1, 2, 3 and 4. A good agreement between experimental and calculated data (symbols and continuous line respectively) has been obtained as it can be seen in figure 4.

The DC conductivity (σ_0) of both grades of polyetherimide increases with the temperature as it can be seen in tables 1 and 2. Figure 6 shows an Arrhenius plot of the conductivity where it can be seen that it is thermally activated. This increase has been attributed to an increase of carrier mobility [13]. It can be fitted to

$$\sigma_0 = \sigma_{0PF} \exp(E_a/kT) \quad (10)$$

The activation energies and preexponential factors can be seen in table 5. Ultem 1000 presents a slightly higher activation energy for the DC conductivity.

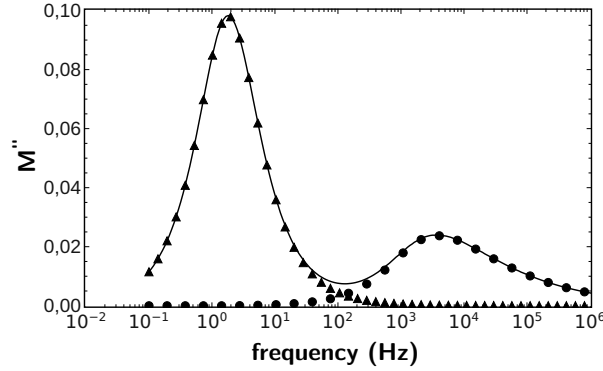


Figure 5. Imaginary part of the electric modulus at $T = 255$ °C of Ultem 1000: line is the value calculated by means of equation 9; symbols indicate the separate contributions of conductive process given by equation 6 (▲) and main relaxation α (●) given by equation 7. Parameters σ_0 , ω_p , $\varepsilon_{\infty C}$, n characterize conductive process, whereas that parameters $\varepsilon_{\infty HN}$, τ_{HN} , α_{HN} and β_{HN} characterize main relaxation α

Table 1. Parameters associated with conductive processes: Ultem 1000 case. All parameters are fit results.

T (°C)	σ_0 ($\Omega^{-1}\text{cm}^{-1}$)	ω_p (s^{-1})	n	$\varepsilon_{\infty C}$
230	0.271×10^{-10}	14.9	0.678	5.00
235	0.490×10^{-10}	59.8	0.596	5.00
240	0.896×10^{-10}	90.8	0.628	4.91
245	0.156×10^{-9}	375.5	0.546	4.92
250	0.272×10^{-9}	787.4	0.524	4.88
255	0.473×10^{-9}	0.590×10^4	0.429	4.88
260	0.803×10^{-9}	0.165×10^5	0.407	4.85
265	0.133×10^{-8}	0.567×10^5	0.344	4.81
270	0.201×10^{-8}	0.552×10^6	0.202	4.76
275	0.345×10^{-8}	0.430×10^6	0.315	4.72
280	0.483×10^{-8}	0.588×10^7	0.144	4.64
285	0.748×10^{-8}	0.726×10^6	0.217	4.00

Concerning the relaxation time associated with space charge relaxation, it has been proposed that the crossover frequency can be associated with a characteristic time τ_p by means of $\tau_p = 2\pi/\omega_p$. Experimental evidence has been given to support the idea that this characteristic time is actually the same time that an average relaxation time $\langle\tau\rangle$ [30], which can be defined in terms of the area under the Kohlrausch-Williams-Watts (KWW) function as

$$\langle\tau\rangle = \int_0^\infty \Phi(t) dt = \frac{\Gamma(1/\beta)\tau^*}{\beta} \quad (11)$$

Table 2. Parameters associated with conductive processes: Ultem 5000 case. All parameters are fit results.

T (°C)	σ_0 ($\Omega^{-1}\text{cm}^{-1}$)	ω_p (s^{-1})	n	$\varepsilon_{\infty C}$
255	0.368×10^{-9}	0.181×10^4	0.526	4.28
260	0.577×10^{-9}	0.204×10^4	0.580	4.25
265	0.904×10^{-9}	0.824×10^4	0.507	4.24
270	0.139×10^{-8}	0.569×10^5	0.373	4.22
275	0.213×10^{-8}	0.144×10^6	0.365	4.17
280	0.322×10^{-8}	0.346×10^6	0.332	4.10
285	0.499×10^{-8}	0.198×10^6	0.381	3.99
290	0.624×10^{-8}	0.120×10^6	0.303	3.72

Table 3. Parameters associated with α relaxation: Ultem 1000 case. All parameters are fit results except $\Delta\varepsilon$ that is calculated through equation 8.

T (°C)	$\varepsilon_{\infty\text{HN}}$	τ_{HN} (s)	α_{HN}	β_{HN}	$\Delta\varepsilon$
230	3.51	0.119	0.655	0.748	1.49
235	3.50	0.189×10^{-1}	0.729	0.627	1.50
240	3.48	0.393×10^{-2}	0.813	0.549	1.43
245	3.46	0.123×10^{-2}	0.865	0.494	1.46
250	3.45	0.377×10^{-3}	0.907	0.462	1.43
255	3.43	0.138×10^{-3}	0.899	0.464	1.45
260	3.40	0.575×10^{-4}	0.922	0.443	1.45
265	3.37	0.245×10^{-4}	0.929	0.436	1.44
270	3.35	0.111×10^{-4}	0.926	0.439	1.41
275	3.32	0.564×10^{-5}	0.925	0.443	1.40
280	3.25	0.291×10^{-5}	0.921	0.435	1.39
285	3.19	0.163×10^{-5}	0.929	0.449	1.30

where τ^* and β are the parameters that define the KWW response function

$$\Phi(t) = \exp[-(t/\tau^*)^\beta] \quad (12)$$

This average relaxation time $\langle\tau\rangle$ corresponds to the Maxwell relaxation time, this is, the time that an out-of-equilibrium conductor needs to reach electrostatic equilibrium. It is related to the DC conductivity according to the expression [12]

$$\langle\tau\rangle = \frac{\varepsilon_0 \varepsilon_\infty}{\sigma_0} \quad (13)$$

We have calculated the values of $\langle\tau\rangle$ and τ_p . An attempt to compare both magnitudes in an Arrhenius plot can be seen in figure 7. As it can be seen, both quantities represent a thermally activated relaxation time of the form

$$\tau = \tau_{\text{PF}} \exp(E_a/kT) \quad (14)$$

Table 4. Parameters associated with α relaxation: Ultem 5000 case. All parameters are fit results except $\Delta\epsilon$ that is calculated through equation 8.

T (°C)	$\epsilon_{\infty\text{HN}}$	τ_{HN} (s)	α_{HN}	β_{HN}	$\Delta\epsilon$
255	3.65	0.781×10^{-3}	0.803	0.365	0.63
260	3.61	0.248×10^{-3}	0.864	0.309	0.64
265	3.59	0.840×10^{-4}	0.845	0.315	0.65
270	3.54	0.367×10^{-4}	0.854	0.284	0.68
275	3.50	0.150×10^{-4}	0.835	0.298	0.67
280	3.43	0.689×10^{-5}	0.822	0.299	0.67
285	3.33	0.356×10^{-5}	0.839	0.284	0.66
290	3.11	0.208×10^{-5}	0.847	0.283	0.61

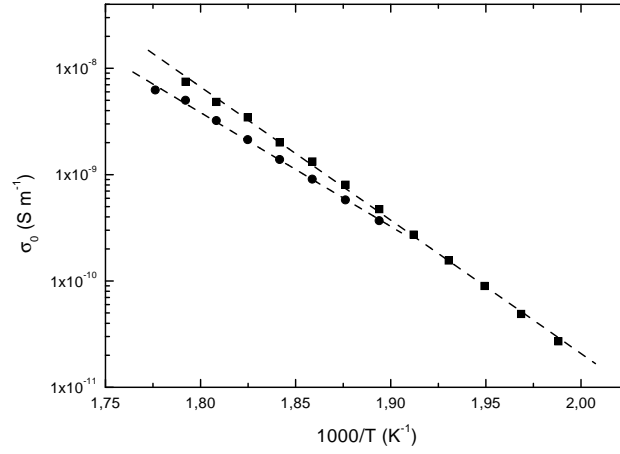


Figure 6. Arrhenius plot of DC conductivity ■, Ultem 1000; ●, Ultem 5000

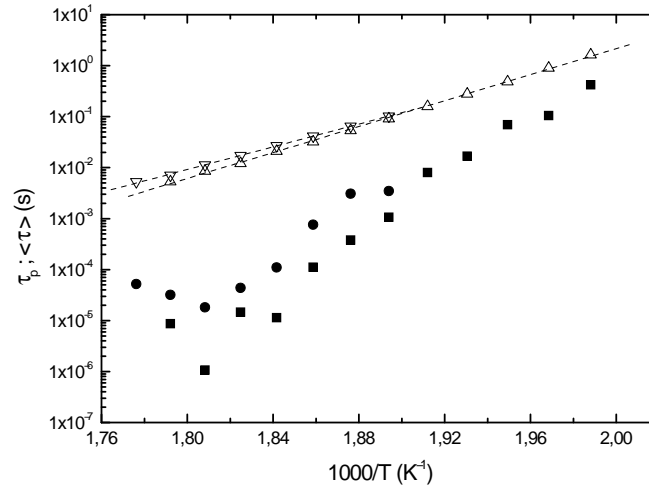


Figure 7. Characteristic time τ_p (associated with crossover frequency $\tau_p = \frac{2\pi}{\omega_p}$): ■, Ultem 1000; ●, Ultem 5000. Maxwell relaxation time $\langle\tau\rangle$: \triangle Ultem 1000; ∇ Ultem 5000

Table 5. Preexponential factors (PF) and activation energies (E_a) of conductivity (σ_0) and relaxation times ($\langle\tau\rangle$ and τ_p), obtained from the corresponding Arrhenius plots

Ultem 1000		
Magnitude	$\log_{10}(PF/1s)$	E_a (eV)
σ_0	14.4	1.08
$\langle\tau\rangle$	-25.1	1.10
τ_p	-56.6 s	2.44
Ultem 5000		
Magnitude	$\log_{10}(PF/1s)$	E_a (eV)
σ_0	10.8	0.92
$\langle\tau\rangle$	-22.1	1.96
τ_p	-58.4	2.56

The activation energies and preexponential factors can be seen in table 5. For both types of relaxation time, the activation energy in the case of Ultem 5000 is higher. It can also be noticed that the activation energy of τ_p is higher than the one of $\langle\tau\rangle$.

It should be clear that these quantities do not represent the same magnitude since their values differ in several orders of magnitude, specially at high temperatures. The agreement between these values was used by León *et al.* to support the hypothesis of a common origin for both DC and AC regimes [30]. Nevertheless, in the following lines we will explain how our results can be reconciled with the idea that both quantities are, at least, related.

In our opinion, the physical meaning of τ_p is just an estimation of the time that separates the relaxation processes for which predominates DC conduction ($\tau > \tau_p$) or predominates AC ($\tau < \tau_p$) conduction.

The mechanism that leads to DC regime are long range displacements [22] where the carriers move in the same direction but at higher frequencies short range hopping of the ion occurs, which is viewed as a correlated motion in which the ion performs several reiterated forward-backward hops before completing any successful forward displacement. Reiterative hopping is the origin of the dispersive regime and it occurs when the frequency is higher than the crossover frequency below which successful hops can be completed.

The high value of $\langle\tau\rangle$ that we have found at high temperatures, in the case of macromolecular materials can be explained on the basis that the microscopic processes that lead to ionic conduction may not be reduced to mere hops over a barrier between adjacent sites. Amorphous polymers, such as PEI, are disordered materials and charge may be located in deep traps. This kind of charge plays a relevant role in microscopic relaxation processes. When the temperature is increased deeply trapped charge may get not enough thermal energy to jump over the potential barrier, but to reach a

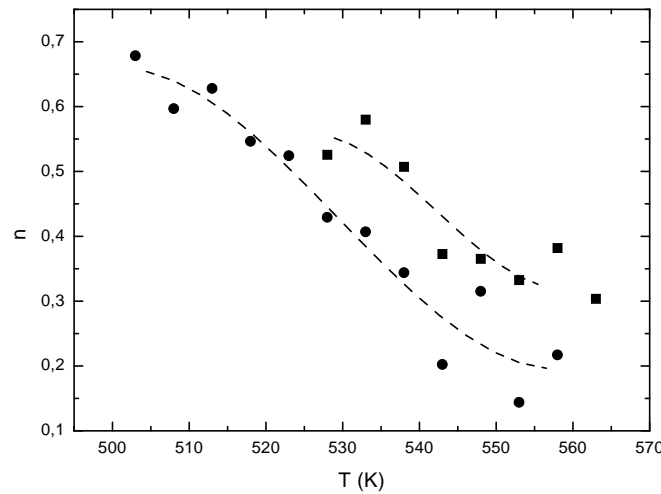


Figure 8. Fractional exponent n as a function of temperature (Dashed lines are a guide for the eye): ■, Ultem 1000; ●, Ultem 5000.

intermediate energy level, resulting in a more complex relaxation behaviour.

If one assumes that the only process that contributes to electrical conduction is hopping, the crossover frequency can be associated with the frequency below which ions can follow the variations of the applied field, so that their characteristic relaxation time is shorter than the applied field period. At such frequencies, DC conductivity determines the relaxation process and, therefore, the Maxwell time determines the crossover frequency.

But if deep traps are present, ions deeply trapped have a longer relaxation time, so that their contribution should be evident at frequencies below the crossover frequency and their effect should represent a slowing down of space charge relaxation process. On the other hand, ions located in deep traps can not follow the field oscillations at higher frequencies and they do not contribute to the relaxation process. Therefore, the presence of deep traps can be associated with a slowing down of the relaxation process, that results in an apparent Maxwell time longer than the relaxation time that corresponds to the crossover frequency. The higher value of $\langle \tau \rangle$ and the higher activation energy of τ_p can thus be explained by the presence of deep traps.

The temperature dependence of the fractional exponent n is shown in figure 8. This parameter characterizes the power-law conduction regime, which is associated with the slowing down of the relaxation process in the frequency domain as a result of the cooperative effects, in the same way as the KWW function does in the time domain. An important connection between these two approaches stems from the coupling model of Ngai and Kannert [34]. This model predicts a power-law conductivity associated with the KWW relaxation function (equation 12) given by

$$\sigma_{\text{KWW}} = B \exp(-E_a/kT) \omega^{1-\beta} \quad (15)$$

Therefore, if any other contribution is sufficiently smaller than that of σ_{KWW} , then

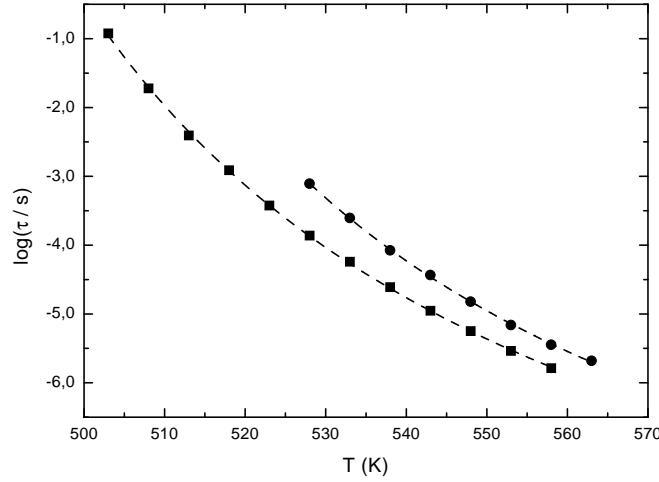


Figure 9. Relaxation time τ_{HN} as a function of temperature: \blacksquare , Ultem 1000; \bullet , Ultem 5000. Dashed lines are curves fitted to VFT equation.

the conductivity of the material may be described by $\sigma_{\text{KWW}}(\omega)$ [34]. In that case, the sublinear dispersive AC conductivity observed in polyetherimide can be associated with a KWW relaxation mechanism with $\beta = 1 - n$ where n is the power-law exponent determined from $\sigma(\omega)$.

The stretched exponential relaxation time has been associated with a slowing of the relaxation process that results from correlated hopping. according to this interpretation, the stretched exponential parameter β represents a correlation index of carrier motion.

One would expect β to be close to zero for strongly correlated systems and close to 1 for random Debye-like hops. As we can see in figure 8 the power-law exponent $n = 1 - \beta$ decreases with temperature for both grades, indicating that correlation of ionic motion decreases with temperature. This can be associated with the increasing disorder due to thermal agitation of polymer chain segments.

In tables 3 and 4 we can see the evolution of the fitting parameters for the α relaxation. The α_{HN} parameter indicates the non-exponentiality of the relaxation. This is, $\alpha_{\text{HN}} = 1$ is a Debye-like relaxation and $\alpha_{\text{HN}} < 1$ indicates that the relaxation extends over a wider range than a Debye relaxation. The non-exponentiality maybe due to a distribution of relaxation times or to cooperativity. As the temperature increases and attains values progressively further from the T_g of the material, the value of α_{HN} is closer to 1. In this case this is due to less cooperativity as the glass transition is left further away. On the other hand, the parameter β_{HN} decreases, which means that a broader range of relaxation modes are excited at temperatures further from T_g , but at the expense of a lower overall dielectrics strength, as it can be seen in the tables. This is analogous to what happens in TSDC when a poling temperature far from the optimal one is employed.

In the case of the α relaxation, figure 9 shows that the relaxation time τ_{HN} decreases

Table 6. Preexponential factors $\tau_{\text{HN}0}$, E_{W} and T_0 obtained by fitting the relaxation time τ_{HN} to VTF equation

Grade	$\tau_{\text{HN}0}$ (s)	E_{W} (eV)	T_0 (K)
ULTEM 1000	1.43×10^{-11}	0.11	446
ULTEM 5000	4.95×10^{-12}	0.12	452

with temperature following the Vogel–Fulcher–Tammann (VFT) equation

$$\tau_{\text{HN}} = \tau_{\text{HN}0} \frac{E_{\text{W}}}{k_{\text{B}}(T - T_0)} \quad (16)$$

for both PEI grades. The result of the fits can be seen in table 6. This behaviour is typical of cooperative non-exponential relaxations. This is not surprising since the α relaxation is related to the glass transition of the material. The value of T_0 is lower in Ultem 1000 than in Ultem 5000. This is logical taking into account that they should follow a pattern similar to T_{g} .

4. Conclusions

Conductive processes in two grades of commercial polyetherimide have been studied and it has been found that they condition the electrical behaviour of these materials at high temperatures and low frequencies. The electric modulus formalism has been useful in order to interpret dynamic electrical analysis data to characterize these processes.

The α relaxation has also been studied due to its proximity to the conductive relaxation that made impossible to study just the conduction on their own.

The dispersive conductivity observed in both grades of polyetherimides can be explained by means of a sublinear frequency dispersive AC conductivity. This behaviour is the result of correlated hopping.

The DC conductivity is thermally activated, probably due to an increase of carriers.

Among the parameters studied, there is the crossover relaxation time τ_{p} . The physical meaning of τ_{p} is just an estimation of the time that separates the relaxation processes for which predominates DC conduction ($\tau > \tau_{\text{p}}$) or predominates AC ($\tau < \tau_{\text{p}}$) conduction.

In the literature [30], experimental evidence of the equivalence of the crossover relaxation time with the Maxwell relaxation time has been presented but in our case the presence of deep traps can produce a slowing down of the relaxation process. This results in an apparent Maxwell time longer than the crossover relaxation time.

Both relaxation times are thermally activated. This is to be expected in the case of the Maxwell relaxation time, since it is calculated from the DC conductivity. In the case of the crossover relaxation time, this fact reinforces the idea that it is physically related to the Maxwell relaxation time. The higher activation energy in the case of the crossover relaxation time can also be attributed to the presence of deep traps.

The power-law exponent n decreases with temperature for both grades, indicating that correlation of ionic motion decreases with temperature. This can be associated with the increasing disorder due to thermal agitation of polymer chain segments.

The behaviour of the α relaxation is typical of cooperative non-exponential relaxations. This is not surprising since the α relaxation is related to the glass transition of the material. As the temperature attains values further to T_g the response from the α relaxation becomes less cooperative even though a broader range of the relaxation is involved.

Acknowledgements

This work has been partially supported by project 2009 SGR 01168 (AGAUR).

References

- [1] N. Zebouchi, V. H. Truong, R. Essolbi, M. Se-Ondoua, D. Malec, N. Vella, S. Malrieu, A. Toureille, F. Schué, and R. G. Jones. The electric breakdown behaviour of polyetherimide films. *Polym. Int.*, 46(1):54–58, 1998.
- [2] E. Krause, G. M. Yang, and G. M. Sessler. Charge dynamics and morphology of Ultem 1000 and Ultem 5000 PEI grade films. *Polym. Int.*, 46(1):59–64, 1998.
- [3] R. Díaz-Calleja, S. Friederichs, C. Jaimes, M. J. Sanchis, J. Belana, J. C. Cañadas, J. A. Diego, and M. Mudarra. Comparative study of mechanical and electrical relaxations in poly(etherimide). part 2. *Polym. Int.*, 46(1):20–28, 1998.
- [4] J. Belana, J. C. Cañadas, J. A. Diego, M. Mudarra, R. Díaz-Calleja, S. Friederichs, C. Jaimes, and M. J. Sanchis. Comparative study of mechanical and electrical relaxations in poly(etherimide). part 1. *Polym. Int.*, 46(1):11–19, 1998.
- [5] R. Chen and Y. Kirsh. *Analysis of thermally stimulated processes*, chapter 2, pages 35–92. Pergamon Press, Oxford, 1981.
- [6] M. Mudarra and J. Belana. Study of poly(methyl methacrylate) space charge relaxation by TSDC. *Polymer*, 38:5815–5821, 1997.
- [7] M. Mudarra, J. Belana, J. C. Cañadas, and J. A. Diego. Polarization time effect on PMMA space charge relaxation by TSDC. *J. Polym. Sci. Pol. Phys.*, pages 1971–1980, 1998.
- [8] M. Mudarra, J. Belana, J. C. Cañadas, and J. A. Diego. Windowing polarization: considerations to study the space charge relaxation in poly(methyl methacrylate) by thermally stimulated depolarization currents. *Polymer*, 40:2659–2665, 1999.
- [9] C. T. Moynihan. Description and analysis of electrical relaxation data for ionically conducting glasses and melts. *Solid State Ionics*, 105:175–183, 1998.
- [10] P. Pissis and A. Kyritsis. Electrical conductivity in hydrogels. *Solid State Ionics*, 97:105–113, 1997.
- [11] J. R. Macdonald. Resolution of conflicting views concerning frequency-response models for conducting materials with dispersive relaxation, and isomorphism of macroscopic and microscopic models. *Solid State Ionics*, 150:263–279, 2002.
- [12] I. M. Hodge, K. L. Ngai, and C. T. Moynihan. Comments on the electric modulus function. *J. Non-Cryst. Solids*, 351:104–115, 2005.
- [13] M. Mudarra, J. Belana, J. C. Cañadas, J. A. Diego, J. Sellarès, R. Díaz-Calleja, and M. J. Sanchis. Space charge relaxation in polyetherimides by the electric modulus formalism. *J. Appl. Phys.*, 88:4807–4812, 2000.

- [14] Hongbo Lu, Xingyuan Zhang, and Hui Zhang. Influence of the relaxation of Maxwell–Wagner–Sillars polarization and DC conductivity on the dielectric behaviors of nylon 1010. *J. Appl. Phys.*, 100:054104(7pp), 2006.
- [15] S. Lanfredi, P. S. Saia, R. Lebullenger, and A. C. Hernandez. Electric conductivity and relaxation in fluoride, fluorophosphate and phosphate glasses: analysis by impedance spectroscopy. *Solid State Ionics*, 146:329–339, 2002.
- [16] A. Rivera, J. Santamaría, and C. León. Electrical conductivity relaxation in thin-film yttria-stabilized zirconia. *Appl. Phys. Lett.*, 78:610–612, 2001.
- [17] Jianjun Liu, Chun-Gang Duan, Wei-Guo Yin, W. N. Mei, R. W. Smith, and J. R. Hardy. Dielectric permittivity and electric modulus in $\text{Bi}_2\text{Ti}_4\text{O}_{11}$. *J. Chem. Phys.*, 119:2812–2819, 2003.
- [18] G. C. Psarras, E. Manolakaki, and G. M. Tsangaris. Dielectric dispersion and AC conductivity in —iron particles loaded— polymer composites. *Compos. Part A–Appl. S.*, 34:1187–1198, 2003.
- [19] M. D. Migahed, M. Ishra, T. Fahmy, and A. Barakat. Electric modulus and AC conductivity studies in conducting PPy composite films at low temperature. *J. Phys. Chem. Solids*, 65:1121–1125, 2004.
- [20] A. K. Jonscher. *Dielectric relaxation in solids*, chapter 5, pages 161–253. Chelsea Dielectric Press, 1983.
- [21] A. K. Jonscher. *Dielectric relaxation in solids*, chapter 8, pages 310–370. Chelsea Dielectric Press, 1983.
- [22] D. L. Sidebottom, P. F. Green, and R. K. Brow. Two contributions to the AC conductivity of alkali oxide glasses. *Phys. Rev. Lett.*, 74:5068–5071, 1995.
- [23] D. L. Sidebottom, P. F. Green, and R. K. Brow. Scaling parallels in the non-debye dielectric relaxation of ionic glasses and dipoles supercooled liquids. *Phys. Rev. B*, 56:170–177, 1997.
- [24] C. León, M. L. Lucía, J. Santamaría, and F. Sánchez-Quesada. Universal scaling of the conductivity relaxation in crystalline ionic conductors. *Phys. Rev. B*, 57 (1):41–44, 1998.
- [25] P. S. Anantha and K. Hariharan. AC conductivity analysis and dielectric relaxation behaviour of $\text{NaNO}_3\text{--Al}_2\text{O}_3$ composites. *Mat. Sci. Eng. B–Solid*, 121:12–19, 2005.
- [26] H. M. Millany and A. K. Jonscher. Dielectric properties of stearic acid multilayers. *Thin Solid Films*, 11:257–273, 1980.
- [27] D. P. Almond, A. R. West, and R. J. Grant. Temperature dependence of the AC conductivity of $\text{Na}\beta\text{--alumina}$. *Solid State Commun.*, 44:1277–1280, 1982.
- [28] H. W. Starkweather Jr. and P. Avakian. Conductivity and the electric modulus in polymers. *J. Polym. Sci. Pol. Phys.*, 30:637–641, 1992.
- [29] J. R. Macdonald. *Impedance Spectroscopy: Emphasizing Solid Materials and Systems*, chapter 2, pages 27–132. Wiley–Interscience, 1987.
- [30] C. León, M. L. Lucía, and J. Santamaría. Correlated ion hopping in single-crystal yttria-stabilized zirconia. *Phys. Rev. B*, 55 (2):882–887, 1997.
- [31] E. Laredo, N. Suarez, A. Bello, and J. M. G. Fatou B. R. de Gáscue, M. A. Gomez. α , β and γ relaxations of functionalized HD polyethylene: a TSDC and a mechanical study. *Polymer*, 40:6405–6416, 1999.
- [32] M. Grimaud, E. Laredo, A. Bello, and N. Suarez. Correlation between dipolar TSDC and AC dielectric spectroscopy at the PVDF glass transition. *J. Polym. Sci. Pol. Phys.*, 35:2483–2493, 1997.
- [33] A. Bello, E. Laredo, and M. Grimaud. Distribution of relaxation times from dielectric spectroscopy using monte carlo simulated annealing: Application to α -PVDF. *Phys. Rev. B*, 60:12764–12774, 1999.
- [34] D. L. Sidebottom, P. F. Green, and R. K. Brow. Comparison of KWW and power law analyses of an ion-conducting glass. *J. Non-Cryst. Solids*, 183:151–160, 1995.